HHS Public Access

Author manuscript

Nature. Author manuscript; available in PMC 2019 September 13.

Published in final edited form as:

Nature. 2019 March ; 567(7749): 521–524. doi:10.1038/s41586-019-1012-y.

Efficacy of MEK Inhibition in Patients with Histiocytic Neoplasms

Eli L. Diamond[1,10,*], **Benjamin H. Durham**[2,3,*], **Gary A Ulaner**[4,10], **Esther Drill**[5], **Justin Buthorn**[1], **Michelle Ki**[3], **Lillian Bitner**[3], **Hana Cho**[3], **Robert J. Young**[4], **Jasmine H Francis**[6], **Raajit Rampal**[7], **Mario Lacouture**[8], **Lynn A. Brody**[4], **Neval Ozkaya**[2,11], **Ahmet Dogan**[2], **Neal Rosen**[7,9,10], **Alexia Iasonos**[5,10], **Omar Abdel-Wahab**[3,7,10,**], and **David M. Hyman**[7,10,**]

[1]Dept. of Neurology, Memorial Sloan Kettering Cancer Center, New York, NY, 10065

[2]Dept. of Pathology, Memorial Sloan Kettering Cancer Center, New York, NY, 10065

[3]Human Oncology and Pathogenesis Program, Dept. of Medicine, Memorial Sloan Kettering Cancer Center, New York, NY 10065

[4]Dept. of Radiology, Memorial Sloan Kettering Cancer Center, New York, NY, 10065

[5]Dept. of Epidemiology and Statistics, Memorial Sloan Kettering Cancer Center, New York, NY, 10065

[6]Ophthalmic Oncology Service, Dept. of Medicine, Memorial Sloan Kettering Cancer Center, New York, NY, 10065

[7]Dept. of Medicine, Memorial Sloan Kettering Cancer Center, New York, NY, 10065

[8]Dermatology Service, Dept. of Medicine, Memorial Sloan Kettering Cancer Center, New York, NY, 10065

[9]Molecular Pharmacology and Chemistry Program, Memorial Sloan Kettering Cancer Center, New York, NY 10065

[10]Weill Cornell Medical College, New York, NY, 10065

[11]Laboratory of Pathology, National Cancer Institute, Bethesda, MD

Abstract

[**]Co-corresponding. **Correspondence:** Omar Abdel-Wahab, Memorial Sloan Kettering Cancer, 1275 York Avenue, New York, NY 10065, +16468883487, abdelwao@mskcc.org, David M. Hyman,, Memorial Sloan Kettering Cancer Center, 1275 York Avenue, New York, NY 10065, +16468884544, hymand@mskcc.org.

[*]These authors contributed equally to this work.

Author contributions ELD, OAW, and DMH designed the study. MK, LB, and HC processed all patient material for isolation of DNA and RNA for genomic analyses. BHD cloned all cDNAs and performed *in vitro* studies of their effects on cell growth and signaling under the supervision of NR and OAW. BHD also analyzed genomic data under the supervision of OAW. JB collected data and samples for processing by MK, LB, and HC. ELD, JHF, RR, ML, and LAB enrolled and treated the patients. ED and AI performed statistical analyses. GAU and EJY evaluated all radiographic studies. ELD, BHD, NO, AD, OAW, and DMH analyzed the clinical and laboratory data. ELD, BHD, OAW, and DMH prepared the manuscript with help from all co-authors.

Supplementary Information available online.

Reviewer Information *Nature* thanks X and the other anonymous reviewer(s) for their contribution to the peer review of this work.

Histiocytic neoplasms are a heterogeneous group of clonal hematopoietic disorders marked by diverse mutations in the mitogen-activated protein kinase (MAPK) pathway.[1,2] For the 50% of histiocytosis patients with BRAFV600-mutations[3–5], RAF inhibition is highly efficacious and has dramatically altered the natural history of the disease.[6,7] Conversely, no standard therapy exists for the remaining 50% of patients lacking BRAFV600-mutations. While ERK dependence has been hypothesized to be a consistent feature across histiocytic neoplasms, this remains clinically unproven and many kinase mutations found in these patients have not been biologically characterized. We set out to evaluate ERK dependence in histiocytoses through a proof-of-concept clinical trial of the oral MEK1/2 inhibitor cobimetinib in patients with histiocytoses. Patients were enrolled regardless of tumor genotype. In parallel, novel MAPK alterations identified in treated patients were characterized for their ability to activate ERK. In 18 treated patients, the overall response rate (ORR) was 89% (90% CI: 73–100). Responses were durable, with no acquired resistance to date. At one year, 100% of responses were ongoing, and 94% of patients remained progression-free. Efficacy was observed regardless of genotype with responses achieved in patients with ARAF, BRAF, RAF1, NRAS, KRAS, MEK1, and MEK2 mutations. Consistent with observed responses, characterization of the novel mutations identified in treated patients confirmed them to be activating. Collectively, these data demonstrate that histiocytic neoplasms are characterized by remarkable dependence on MAPK signaling and, consequently, responsiveness to MEK inhibition. These results extend the benefits of molecularly targeted therapy to the entire spectrum of patients with histiocytosis.

Based on the success of targeting BRAFV600 in the two most common histiocytic neoplasms, Langerhans cell histiocytosis (LCH) and Erdheim-Chester disease (ECD), efforts were undertaken to identify potential genomic drivers of disease in patients that do not harbor this mutation. These genomic studies of histiocytoses have identified a remarkable diversity of both previously characterized as well as novel alterations involving multiple components of the MAPK pathway[8–13]. Interestingly, many of the recurrent mutations in histiocytic neoplasms occur in MAPK pathway genes such as ARAF, RAF1, MEK1, and MEK2 that are rarely, if ever, mutated in other malignancies. Consequently, many of these mutations have not been biologically characterized. Consistent with the underlying hypothesis that these non-BRAFV600 mutations likely drive histiocytic neoplasms, drugs that inhibit both MEK1/2, kinases immediately downstream of BRAF, have been shown in case reports to evoke responses in these patients[14–16]. Despite these findings, the true extent and durability of response, as well as safety of MEK1/2 inhibition across a wider range of histologic and molecular subsets of histiocytosis remains unknown.

To formally evaluate the therapeutic potential of MEK1/2 inhibition in histiocytic neoplasms, we conducted a Phase II study of the MEK1/2 inhibitor, cobimetinib, in adult patients with histiocytoses of any mutational status (ClinicalTrials.gov, NCT02649972). Consistent with common clinical practice for response assessment in these disorders[17–19], the primary endpoint was response rate (complete response + partial response) as determined by fluorodeoxyglucose (FDG)-positron emission tomography (PET). To provide additional corroboration of treatment efficacy, a key secondary end point included response by CT/MRI per RECIST version 1.1[20]. Simultaneously, we utilized this clinical trial as a platform to perform real-time patient-driven discovery of novel MAPK pathway alterations

through biological characterization of novel alterations identified through comprehensive profiling of patient samples.

A total of 18 patients were enrolled and treated (Extended Data Table 1). Patients had a variety of histiocytic neoplasms including ECD (n=12 patients), LCH (n=2), Rosai-Dorfman disease (n=2), and mixed histiocytosis (n=2). Eighty-nine percent (16/18) of patients had received at least one prior therapy and 56% (10/18) two or more prior therapies. Five patients (28%) had an ECOG performance status of ≥2.

At the time of the pre-planned primary efficacy analysis performed using a data-cutoff of April 25, 2018, the ORR was 89% (90% one-sided confidence interval [CI], 73 to 100), as determined by PET response criteria (Fig. 1a). Overall, 72% of the patients (13 patients) had a complete response, 17% (3) partial response, 6% (1) stable disease, none (0) had progressive disease, and 6% (1) could not be evaluated owing to early withdrawal for clinical deterioration (Extended Data Table 2). All patients were accounted for in the analysis, including the patient who could not be evaluated, per protocol (counted as non-responder). Responses occurred at all sites of disease including the central nervous system, a site associated with morbidity and mortality[21]. According to CT/MRI-based RECIST v1.1 criteria, the ORR was 57% (90% one-sided CI: 37 to 100), in the 14 of 18 patients evaluable by these criteria (Extended Data Fig. 1). The median time to best response according to PET response criteria was 3.2 months (range, 1.6 to 15.9, Fig. 1b). At the time of data analysis, 50% (9/18) of patients remained on protocol therapy, and an additional 17% (3/18), all in complete response, had elected to withdraw and continue to receive MEK inhibitory therapy off-label.

The median duration of response and the median progression-free survival had not yet been reached after a median follow up of 11.9 months (range, 4.6 to 26.4) (Fig. 1c, Extended Data Fig. 2). No responding patient has progressed to date. Among those who discontinued treatment for any reason, median time on treatment was 11.9 months (range, 1.6 to 23.7). At one year, 100% of responses were ongoing, and 94% of patients remained progression-free.

The adverse events observed are shown in Extended Data Table 3-4. Overall, the safety profile was consistent with prior studies of cobimetinib[22,23]. Of the 18 treated patients, 10 (56%) had their cobimetinib dose reduced at least once. Adverse events leading to dose reduction included ejection fraction decrease (in 5 patients), rash (in 2), diarrhea (in 2), and fatigue and thrombocytopenia (in 1 each). In all cases, patients whose doses were reduced had their best response maintained at the lower dose. One patient permanently discontinued cobimetinib due to an adverse event (central retinal vein occlusion). Another patient with extensive baseline histiocytic lung involvement died of pneumonia, deemed unrelated to cobimetinib, prior to first response assessment and was counted as a non-responder per protocol.

To identify the MAPK pathway alterations present in each patient, a variety of sequencing assays were performed according to tissue availability (Extended Data Table 5). In some cases, MAPK mutations were defined on the basis of sequencing performed at an outside commercial laboratory. At least one mutation involving the MAPK pathway was identified

in 83% (15/18) of patients. Patients harbored a variety of MAPK pathway mutations involving BRAF (n=5 with V600, n=1 with non-V600), MEK1 (n=4), KRAS (n=3), ARAF (n=2), RAF1 (n=1), MEK2 (n=1), and NRAS (n=1). Two patients had mutations involving more than one gene in the MAPK pathway. Three patients had unknown mutational status, including one case in which sequencing of two separate biopsies failed due to low tumor cellularity. Responses were observed across genotypes, as well as in 2 of 3 patients with unknown mutations (Fig. 1a). While several alterations detected here (including several in BRAF, ARAF, and MEK1) are known to be recurrent in histiocytoses, RAF1 mutations have not been previously described in histiocytoses, and the specific RAF1, MEK2, and BRAF indel mutations identified here have not been functionally characterized in any setting (Extended Data Fig. 4). We therefore evaluated the transforming potential, ability to activate ERK, and responsiveness to cobimetinib *in vitro* for each of these three novel mutations. In each case, the MEK2 Y134H, BRAF N486_T491delinsK, and RAF1 K106N mutations robustly led to cytokine independence in Ba/F3 cells (a murine IL3-dependent, pro-B cell line) and activated ERK signaling while wild-type MEK2, RAF1, and BRAF did not (Fig. 2a-f). Moreover, expression of each mutation sensitized Ba/F3 cells to cobimetinib while parental Ba/F3 cells remained relatively insensitive to cobimetinib (Fig. 2g). These *in vitro* responses were consistent with the clinical responses seen in patients bearing these same alleles on the trial (Fig. 1a-b and 2a,c,e).

In this study, cobimetinib, a selective inhibitor of MEK1/2, had marked and durable activity in adults with histiocytic neoplasms. Responses to cobimetinib were observed across histiocytosis subtypes and tumor genotypes, although consistent with the expectations for a study mandating adult patients to have either refractory or multiorgan disease, ECD constituted the majority (67%) of treated patients. Therefore, some caution is warranted when applying these findings to all patients with histiocytosis. The efficacy of cobimetinib across MAPK genotypes here is remarkable given that single-agent efficacy of MEK1/2 inhibitors in other MAPK pathway altered solid tumors has generally been disappointing[24]. Indeed, prior work has shown that RAS mutations vary in their dependence on MEK1/2[25,26]. Similarly, preclinical studies have previously suggested that several MEK1/2 mutations, including some observed in patients treated here, would confer resistance to MEK1/2 inhibition[27,28]. Importantly, responses to cobimetinib were not only nearly universal but also durable and, in fact, no acquired resistance has been observed to date. This finding suggests that histiocytic neoplasms may lack the ability to adapt to the tonic MEK1/2 inhibition and suggest that cobimetinib may dramatically alter the natural history of these disorders. It is noteworthy that similar efficacy and durability of response was previously observed with vemurafenib in the subset of histiocytic neoplasms that harbor BRAFV600 mutations[6,7].

Overall, our data demonstrate that cobimetinib results in consistent and durable responses across clinical and genetic subtypes of histiocytic neoplasms, an area of unmet medical need. These findings further suggest that histiocytic neoplasms are collectively characterized by dependence on MAPK pathway signaling and, consequently, responsiveness to MEK1/2 inhibition.

Methods

Patients

Eligible patients had a histiocytic neoplasm, were age 16 or older, had an Eastern Cooperative Oncology Group performance-status score of 0 to 3 (on a scale from 0 to 5, with higher scores indicating greater disability), and had adequate major organ function. Patients were required to have one of the following: (1) multi-system disease, (2) disease that was recurrent or refractory to standard therapies, or (3) single-organ system disease deemed unlikely to benefit from conventional therapies (for example, central nervous system or cardiac infiltration). Patients with tumors that were wild type for BRAF V600 were eligible. Patients with BRAF V600-mutations were eligible only in the setting of (1) intolerance or resistance to prior BRAF inhibitor therapy, or (2) the inability to access BRAF inhibitor therapy. Complete eligibility criteria are available in the study protocol (see Supplemental Information).

The protocol was approved by the institutional review board at Memorial Sloan Kettering Cancer Center, complied with the International Ethical Guidelines for Biomedical Research Involving Human Subjects, Good Clinical Practice guidelines, and the Declaration of Helsinki. All patients provided written informed consent.

Study Design and Treatment

The primary endpoint was the overall response rate (CR + PR) by PET response criteria (see Supplementary Information). These criteria were previously utilized for analysis of vemurafenib efficacy in BRAF V600-mutant histiocytic disorders, a dataset that formed the basis of regulatory authorization for this indication in the United States[7]. PET responses were investigator assessed by a radiologist with dual board-certification in diagnostic radiology and nuclear medicine (GU). Secondary endpoints included duration of response and progression-free survival based on PET criteria, safety and response rate according to the Response Evaluation Criteria in Solid Tumors (RECIST), version 1.1. Patients received cobimetinib at a starting dose of 60mg daily for 21 days of each 28 day cycle.

Study Assessments

Tumor assessments were performed by means of PET/CT, MRI, or clinical measurement with calipers in the case of cutaneous lesions, at baseline, every 8 weeks for 6 months, and every 16 weeks thereafter until disease progression. Adverse events were assessed from the date that informed consent was obtained until at least 28 days after the last dose of cobimetinib was administered. Adverse events were classified and graded according to the Common Terminology Criteria for Adverse Events (CTCAE), version 4.0 (https://evs.nci.nih.gov/ftp1/CTCAE/About.html).

Study Oversight

The study was designed jointly by the first and last authors. The investigators collected and analyzed the data. All authors had access to the data, and the first and last authors wrote the first draft of the manuscript. All the authors were involved in the data analysis and manuscript preparation. All the authors vouch for the completeness and accuracy of the data

and analyses and for the adherence to the study protocols. All the authors made the decision to submit the manuscript for publication. Data, safety, and quality monitoring were performed by the Memorial Sloan Kettering Cancer Center Data and Safety Monitoring Committee. All data elements were de-identified by removing identifying characteristics and replacing them with code numbers 1 through 18.

Statistical Analysis

All the analyses were conducted in accordance with the pre-specified statistical plan as outlined in the protocol unless otherwise indicated (see Supplementary Information). The primary analysis, presented here, was performed at the time the first 18 consecutively enrolled patients to receive cobimetinib were evaluable for response or discontinued protocol therapy (Extended Data Fig. 4). Patients who discontinued therapy without a post-baseline tumor assessment were considered to be non-responders. Assuming a binary endpoint of PET response (complete response or partial response versus neither), we estimated that a sample of 18 patients would provide the study with 90% power to test the hypothesis that the response rate is promising (defined as 35% or higher) against a non-promising rate of 10% or lower. Using an exact, one-sample test for binomial proportion, with Type I error=10% and Type II error=10%, the above rates provided a sample size of 18 patients; if at least 4/18 responses were observed then this would be considered a positive study (i.e. conclude that the true response rate is >10%). Ruling out a lower limit of 10% for the overall response rate was considered to be clinically meaningful in light of the poor response to treatment in the context of multi-system or refractory histiocytosis. Secondary end points included overall response rate according to RECIST version 1.1 and duration of response and progression-free survival (PFS) based on PET criteria as estimated by the Kaplan-Meier method. Duration of response was defined beginning with the date of response and ending with the date of progression, beginning of an alternative anti-cancer (non-MEK inhibitor) therapy, or death, or date of last follow up. PFS was defined as the time from the first day of study treatment, until the first documented progression of disease or death from any cause, whichever occurs first, or date of last follow up. Patients who discontinued cobimetinib, in the absence of progression, in order to receive an off-label MEK inhibitor were censored for DOR and PFS at the at the last follow up date. These patients were also considered to be continuing treatment for the purposes of calculating treatment duration exposure. FDG-PET and RECIST responses were investigator-assessed. All patients who received at least one dose of cobimetinib were included in both the efficacy and safety analysis set. All statistical analyses were performed with R, version 3.5.0 (http://www.R-project.org/)

Genomic Analysis

In patients with samples available for centralized testing, genomic analyses for MAPK pathway mutations was performed on DNA extracted from histiocyte tissue biopsies using a variety of assays, most commonly targeted exon sequencing using MSK-IMPACT or Heme-PACT[29,30]. Targeted RNA sequencing was also utilized for the purposes of detecting gene fusions using the Archer FusionPlex Custom Solid Panel[31]. Whole exome sequencing was also performed, based on DNA adequacy, using fingernails as germline control per previously described methods[8]. In some cases, different biopsies from the same individual

were utilized for different genomic assays. Histiocytic neoplasms are routinely characterized by low tumor cellularity often resulting in low variant allele fractions for established driver mutations such as BRAF V600 [8]. As such, sequences from samples in which no MAPK pathway mutation was called using established pipelines developed and optimized for use in more cellular solid tumors were manually curated and high confidence mutations with lower read support salvaged.

Plasmids

To investigate the functional roles and the activation of oncogenic signaling pathways, we cloned the *MAP2K2* Y134H, *RAF1* K106N, and *BRAF* N486_T491delinsK mutations and expressed them in Ba/F3 cells. MSCV-based expression vectors with GFP and the full-length *MAP2K2*, *RAF1*, and *BRAF* wild type were used as controls. Mutational constructs were cloned into the MSCV-IRES-GFP backbone and checked by digestion and sequencing.

Western Blotting

Anti-phospho-p44/42 MAPK (ERK1/2) (Thr202/Tyr204) (no. 9101), anti-p44/42 MAPK (ERK1/2) (137F5) (no. 4695), anti-MEK1/2 (47E6) (no. 9126), anti-B-Raf (D9T6S) (no. 14814), anti-c-Raf (D4B3J) (no. 53745), as well as the secondary antibodies anti-rabbit IgG-HRP (no. 7076) and anti-mouse IgG-HRP (no. 7074) were purchased from Cell Signaling Technology. Anti-β-Actin (A5441) was purchased from Sigma-Aldrich®. Cell lysates were prepared in RIPA buffer supplemented with Halt protease and phosphatase inhibitor cocktail (Thermo Scientific). Equal amounts of protein, as measured by the BRADFORD protein assay, were resolved in 4–12% Bis-Tris NuPage gradient gels (Life Technologies), and transferred electrophoretically on a polyvinylidene difluoride 0.45-m membrane. Membranes were blocked for 1 h at room temperature in 5% bovine serum albumin (BSA) in TBST before being incubated overnight at 4°C with the primary antibodies. All primary antibodies were diluted 1:1,000 in 5% BSA in TBST, except anti-β-actin, which was diluted 1:5,000 in 5% BSA in TBST. After three washes of 10 min in TBST, secondary antibodies were diluted 1:2,000 in 5% BSA in TBST and incubated for 1 h at room temperature. After another three washes in TBST, detection of the signal was achieved by incubating the membrane on an ECL solution from Millipore and exposure on autoradiography films from Denville Scientific (Metuchen, NJ, USA).

Drug Studies

Cobimetinib was purchased from Selleckchem. Drug studies were conducted *in vitro* using FACS-sorted, DAPI − eGFP + Ba/F3 cells that stably expressed the MIGII-EV, MIGII-MEK2^{Y134H}, MIGII-RAF1 K106N and MIGII-BRAF N486_T491delinsK constructs using the CellTiter-Glo Luminescent Cell Viability Assay from Promega Corporation, according to the manufacturer's instructions. The MIGII-MEK2 Y134H, MIGII-RAF1 K106N, and MIGII-BRAF N486_T491delinsK, FACS-sorted Ba/F3 cells were maintained in RPMI + 10% FBS + penicillin and streptomycin media without murine IL3. Meanwhile, MIGII-EV was maintained in RPMI + 10% FBS + penicillin and streptomycin with recombinant murine IL3 (1 ng/mL).

Data Availability

All datasets generated during and/or analyzed during the current study, including patient-level clinical data as well as all sequencing data have been deposited and are publicly available in the cBioPortal for Cancer Genomics under the accession code 'Histiocytosis Cobimetinib MSK, Nature 2019' (http://www.cbioportal.org/study?id=histiocytosis_cobi_msk_2019).

Extended Data

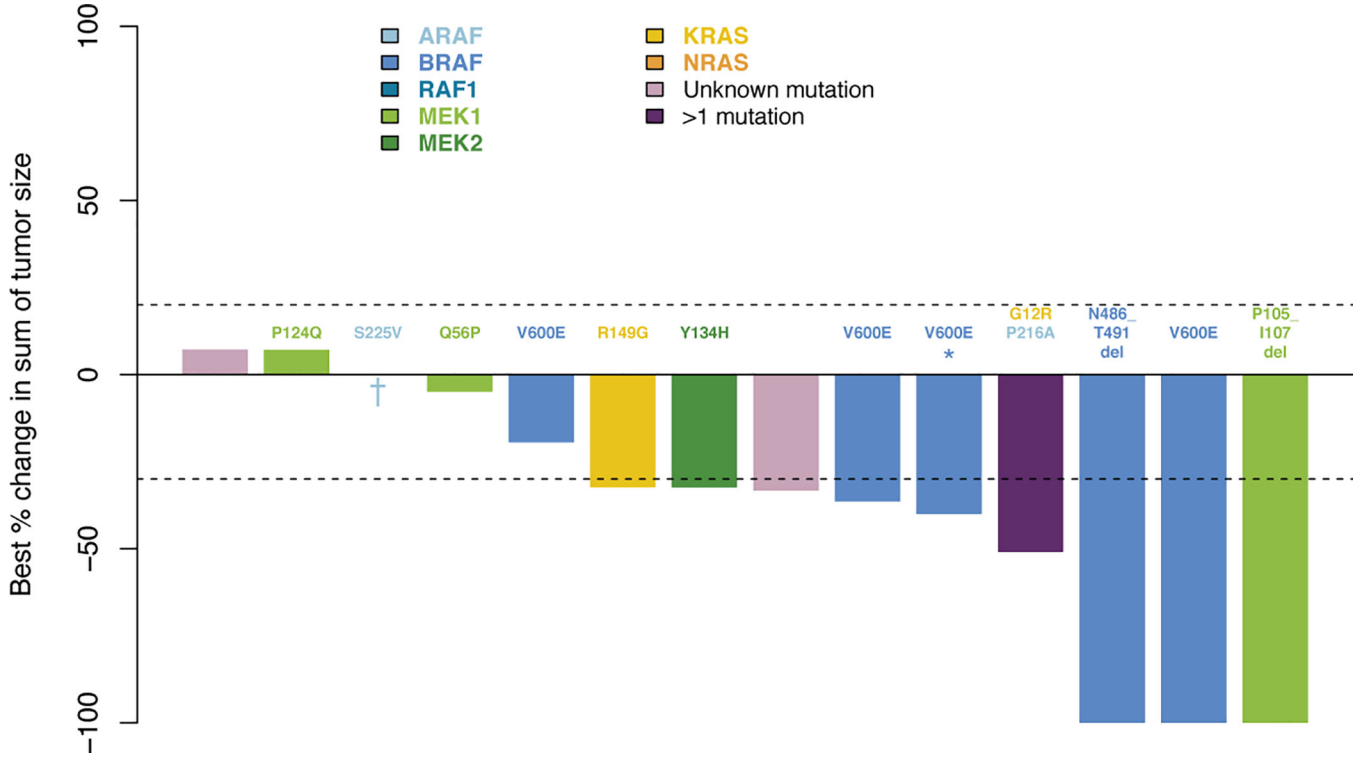

Extended Data Figure 1. Waterfall plot of maximum change in tumor size by RECIST following cobimetinib treatment in histiocytosis patients (n=14).

The upper and lower dotted lines represent cut-offs for progressive disease and partial response, respectively. Colors of bars indicate genomic alteration present. Notations above bars indicate specific mutation. One patient (asterisk) had prior BRAF inhibitor therapy that was discontinued due to intolerance. One patient (dagger) died due to underlying disease.

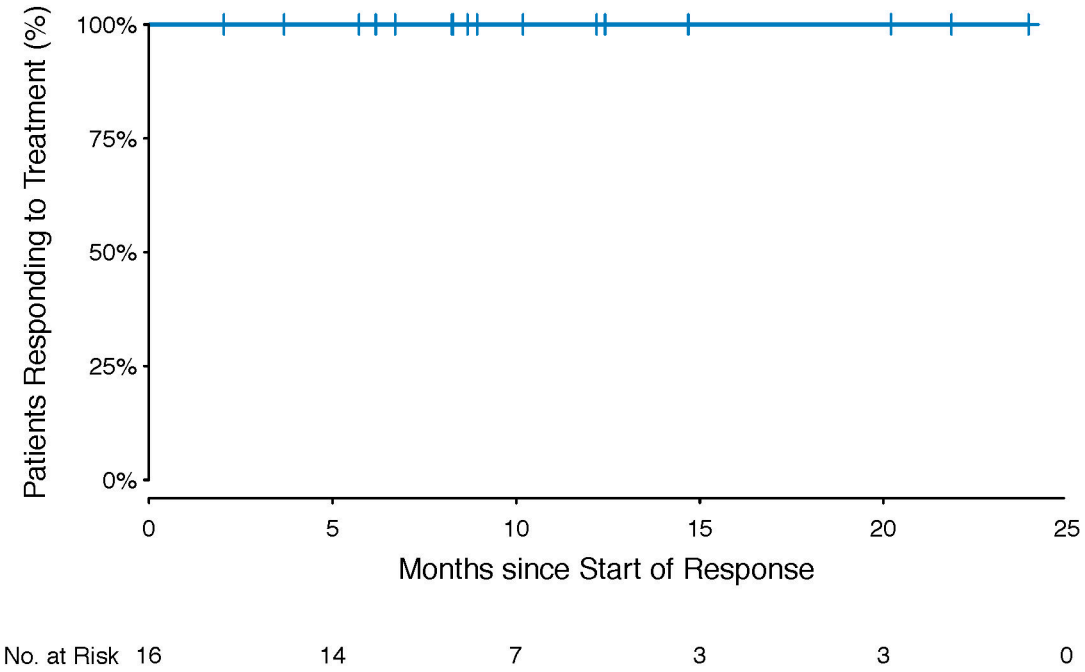

Extended Data Figure 2. PET-Defined Duration of Response (N=16).

Depicts the duration of response according to PET criteria in the 16 responding patients, beginning with date of initial response.

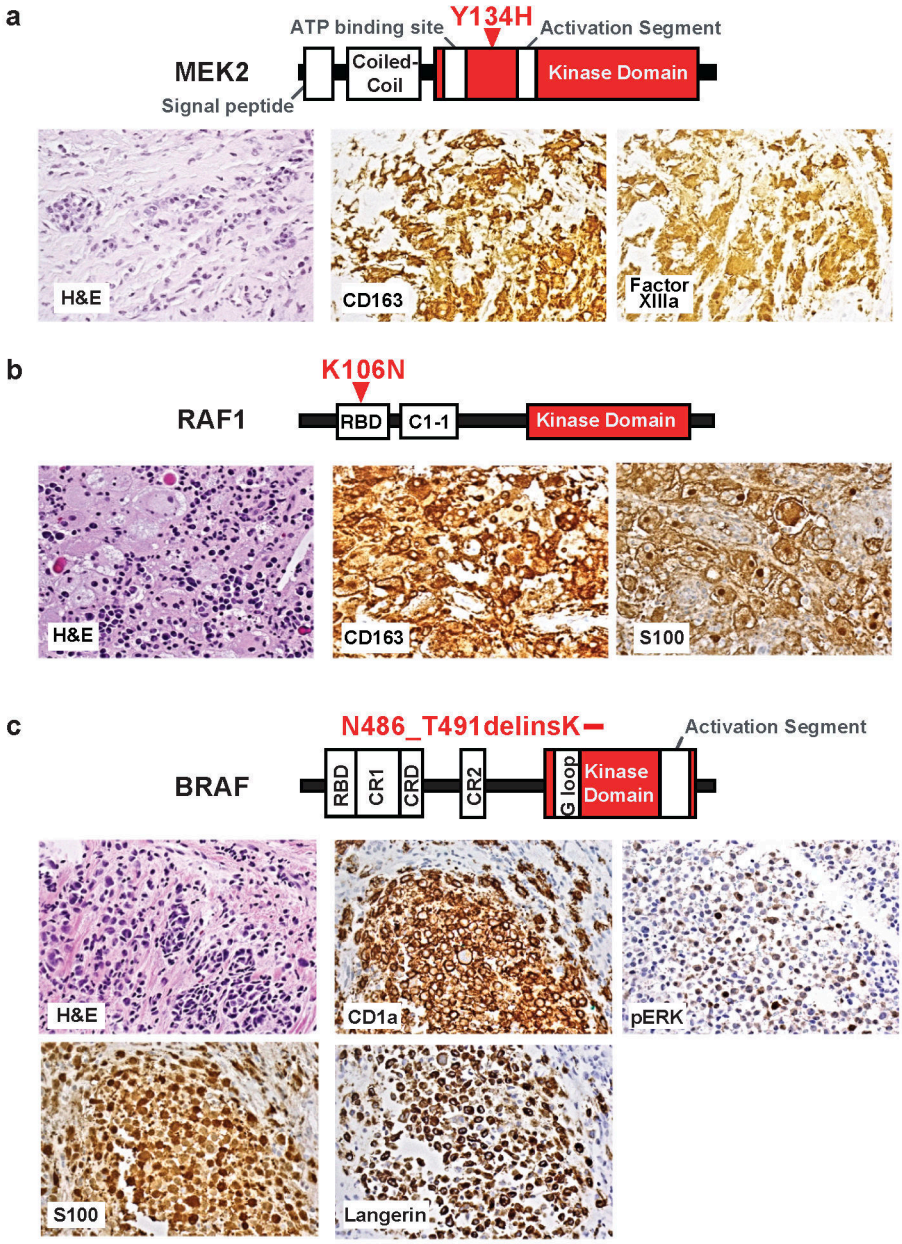

Extended Data Figure 3. Histopathology of histiocytoses with novel activating mutations in MEK2, RAF1, and BRAF treated on study.

(a) Protein diagram (top) and histological images (middle) demonstrating Erdheim-Chester disease (ECD) with a MAP2K2 Y134H mutation. **(b)** Protein diagram (top) and histological images (middle) demonstrating non-Langerhans cell histiocytosis with a RAF1 K106N mutation. **(c)** Protein diagram (top) and histological images (middle) demonstrating ECD with a BRAF N486_T491delinsK mutation.

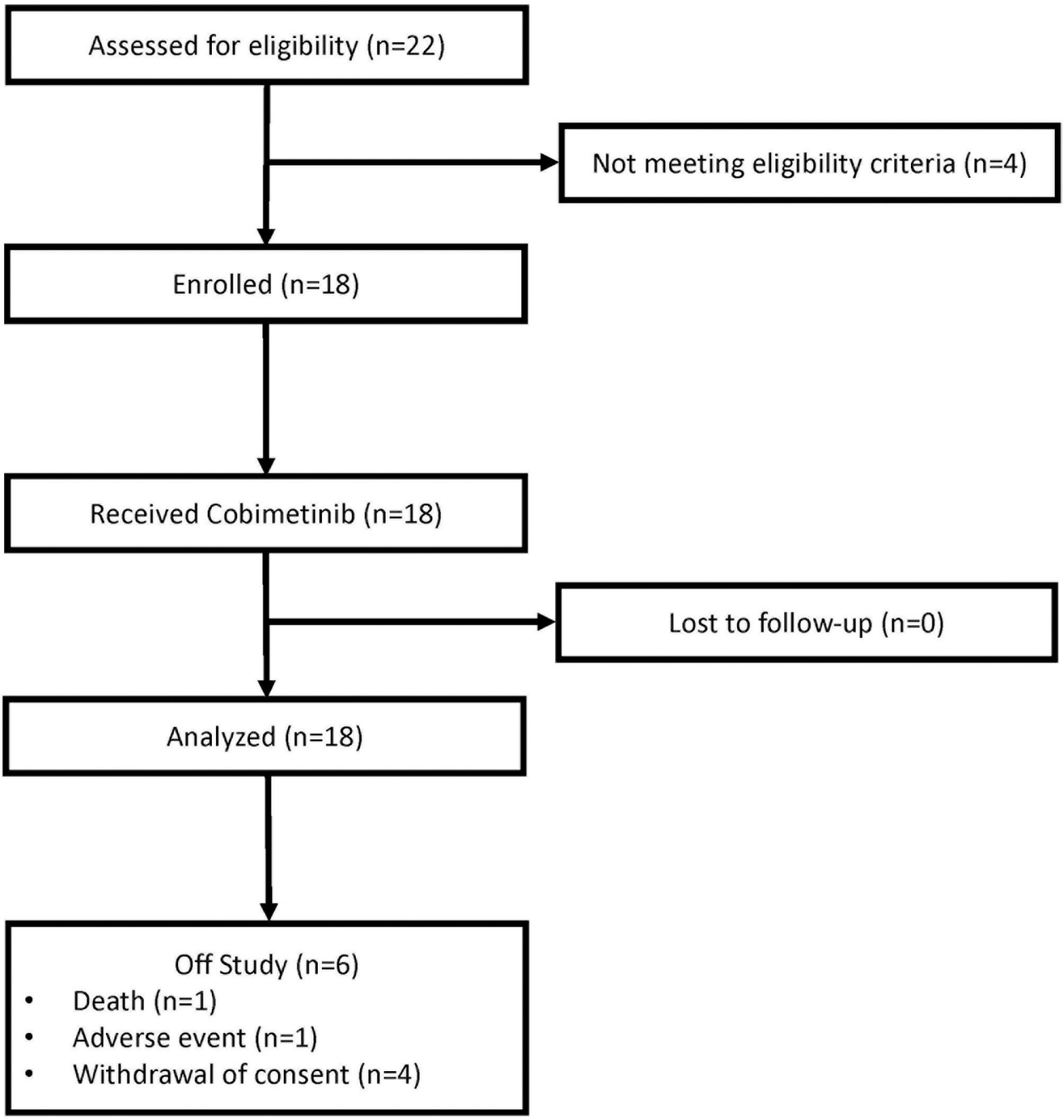

Extended Data Figure 4. Study CONSORT diagram.

Shows the flow of patients through all phases of study participation from enrollment, follow-up, and data analysis.

Extended Data Table 1.

Demographic and Clinical Characteristics (N=18)

Characteristic	Value, N (%)
Age, Median (range) year	51.9 (18.3–79.5)
Sex	
Male	13 (72)
Female	5 (28)
Histiocytosis type	
Erdheim-Chester disease	12 (67)
Rosai-Dorfman disease	2 (11)
Langerhans cell histiocytosis	2 (11)
Mixed histiocytosis	2 (11)
Mitogen-activated protein kinase mutation	
BRAF	
V600E	4 (22)
N486_T491delinsK	1 (6)
MEK1	
Q56P	1 (6)
P105_1107del	1 (6)
P124L	1 (6)
P124Q	1 (6)
ARAF	
S225V	1 (6)
RAF1 K106N	1 (6)
MEK2 Y134H	1 (6)
KRAS R149G	1 (6)
>1 mutation	
BRAF V600E; NRAS G12D; KRAS G13C	1 (6)
KRAS G12R; ARAF P216A	1 (6)
Unknown	3 (17)
ECOG performance-status score	
0	5 (28)
1	8 (44)
2	2 (11)
3	3 (17)
Central nervous system involvement	
Yes	9 (50)
No	9 (50)
No. of prior systemic therapies	
0	2 (11)

Characteristic	Value, N (%)
1	6 (33)
2	8 (44)
≥3	2 (11)
Prior systemic therapy	
Any prior therapy	16 (89)
Immunosuppression[1]	12 (67)
Cytotoxic chemotherapy[2]	9 (50)
Interferon-alpha	5 (28)
Kinase inhibitor[3]	3 (18)

1- Corticosteroids, anakinra, sirolimus, infliximab, intravenous immunoglobulin, rituximab.

2- Methotrexate, cytarabine, cladribine, 6-mercaptopurine, vinblastine, lenolidamide, cyclophosphamide, etoposide.

3- Vemurafenib, dasatinib.

Extended Data Table 2.

Overall Response Rate

Response	PET Response (N=18)	RECIST Response (N=14)
Overall response rate, % (90% one-sided Confidence Interval)	89 (73–100)	57 (37–100)
Best Response, N (%)		
Complete	13 (72)	2 (14)
Partial	3 (17)	6 (43)
Stable	1 (6)	5 (36)
Progressive	0 (0)	0 (0)
Not Evaluable	1 (6)	1 (7)

Demonstrates the overall response rate, and best response (complete, partial, stable, progressive, non-evaluable) using both PET response criteria and RECIST version 1.1 criteria.

Extended Data Table 3.

Safety of cobimetinib in phase 2 study in histiocytosis patients

	Grade 1/2(%)	Grade 3/4 (%)	All (%)
Rash *	15 (83)	0 (0)	15 (83)
Diarrhea	11 (61)	2 (11)	13 (72)
Creatine phosphokinase elevation	10 (56)	1 (6)	11 (61)
Hypomagnesemia	10 (56)	0 (0)	10 (56)
Alkaline phosphatase increased	9 (50)	0 (0)	9 (50)
AST/ALT elevation	8 (44)	0 (0)	8 (44)
Nausea	7 (39)	0 (0)	7 (39)
Anemia	4 (22)	2 (11)	6 (33)
Dry skin	5 (28)	0 (0)	5 (28)
Infection #	5 (28)	0 (0)	5 (28)

	Grade 1/2(%)	Grade 3/4 (%)	All (%)
Vomiting	5 (28)	0 (0)	5 (28)
Abdominal disturbance	4 (22)	0 (0)	4 (22)
Edema limbs	4 (22)	0 (0)	4 (22)
Fatigue	4 (22)	0 (0)	4 (22)
Hyponatremia	2 (11)	2 (11)	4 (22)
Anorexia	3 (17)	0 (0)	3 (17)
Hypoalbuminemia	3(17)	0(0)	3(17)
Hypocalcemia	3 (17)	0 (0)	3 (17)
Pruritus	3 (17)	0 (0)	3 (17)
Serum amylase increased	2 (11)	1 (6)	3 (17)
White blood cell decreased	3 (17)	0 (0)	3 (17)
Hypokalemia	0 (0)	2 (11)	2 (11)
Lipase increased	1 (6)	1 (6)	2 (11)
Lymphocyte count decreased	0 (0)	1 (6)	1 (6)
Retinal vein occlusion	0 (0)	1 (6)	1 (6)

◊Adverse events listed here are those that were attributed by investigators as related to cobimetinib and occurred in at least 15% of patients, regardless of grade, or of any frequency, for grade ≥3.

*Combines the following terms: Rash acneiform, rash maculo-papular.

#Combines the following terms: bladder infection, bronchial infection, oral infection, tooth infection, upper respiratory infection, urinary tract infection, infections - other.

Extended Data Table 4.

Safety, Regardless of Attribution

	Grade 1/2, N (%)	Grade ≥3, N (%)	All, N (%)
Hyperglycemia	15 (83)	1 (6)	16 (89)
Infection	14 (78)	1 (6)	15 (83)
Rash	15 (83)	-	15 (83)
Hypoalbuminemia	14 (78)	-	14 (78)
Diarrhea	11 (61)	2 (11)	13 (72)
Anemia	9 (50)	2 (11)	11 (61)
CPK increased	10 (56)	1 (6)	11 (61)
Hypomagnesemia	11 (61)	-	11 (61)
Alkaline phosphatase increased	10 (56)	-	10 (56)
Hypernatremia	10 (56)	-	10 (56)
AST/ALT increased	9 (50)	1 (6)	10 (56)
Platelet count decreased	8 (44)	2 (11)	10 (56)
White blood cell decreased	7(39)	1 (6)	8 (44)
Edema limbs	7(39)	-	7(39)
Hypocalcemia	5(28)	2 (11)	7(39)
Lipase increased	5(28)	2 (11)	7(39)

	Grade 1/2, N (%)	Grade ≥3, N (%)	All, N (%)
Nausea	7(39)	-	7(39)
Dry skin	6 (33)	-	6 (33)
Fatigue	5(28)	-	5(28)
Hyperkalemia	4(22)	1 (6)	5(28)
Hypoglycemia	5(28)	-	5(28)
Hyponatremia	2 (11)	3(17)	5(28)
Neutrophil count decreased	4(22)	1 (6)	5(28)
Serum amylase increased	4(22)	1 (6)	5(28)
Vomiting	5(28)	-	5(28)
Blood bilirubin increased	4(22)	-	4(22)
Constipation	4(22)	-	4(22)
Dyspnea	3(17)	1 (6)	4(22)
Gastrointestinal symptoms	4(22)	-	4(22)
Lymphocyte count decreased	-	4(22)	4(22)
Pain	3(17)	1 (6)	4(22)
Anorexia	3(17)	-	3(17)
Creatinine increased	3(17)	-	3(17)
Dry mouth	3(17)	-	3(17)
Hypertriglyceridemia	3(17)	-	3(17)
Hypokalemia	1 (6)	2 (11)	3(17)
INR increased	2 (11)	1 (6)	3(17)
Pruritus	3(17)	-	3(17)

[0]Adverse events listed here are those that occurred in at least 15% of patients, regardless of grade or investigator attribution. Infection combines the following terms: bladder infection, bronchial infection, oral infection, tooth infection, upper respiratory infection, urinary tract infection, infections and infestations - other. Rash combines: rash acneiform, rash maculo-papular.

Extended Data Table 5.

Genomic Testing Methodology

Study ID	Histiocytosis	MAPK Pathway Mutation	Assays
1	ECD	ARAF S225V	WES, TES
2	RDD	No mutation identified	None
3	ECD	KRAS R149G	WES, TES
4	RDD	No mutation identified	WES, TES, TRS
5	ECD	BRAF V600E	PCR
6	ECD	BRAF V600E	TES, TRS, cfDNA
7	ECD	BRAF V600E	WES, PCR
8	ECD	BRAF V600E	PCR
9	LCH	BRAF N486_T491del	WES, TES, TRS
10	Mixed Histiocytosis	RAF1 K106N	WES, TES, TRS

Study ID	Histiocytosis	MAPK Pathway Mutation	Assays
11	Mixed Histiocytosis	MEK1 P124L	WES, TES, TRS, Sequenom
12	ECD	MEK1 P124Q	WES, TES, TRS
13	ECD	MEK1 Q56P	WES, TES
14	ECD	MEK1 P105_I107del	WES, TES
15	ECD	MEK2 Y134H	WES, TES, cfDNA
16	ECD	KRAS G12R / ARAF P216A	TES
17	LCH	BRAF V600E / NRAS G12D / KRAS G13C	TES
18	ECD	No mutation identified	WES, TES

ECD: Erdheim-Chester disease; LCH: Langerhans cell histiocytosis; RDD: Rosai-Dorfman disease; CR: complete response; PR: partial response; SD: stable disease; TES: Targeted Exon Sequencing; TRS: Targeted RNA Sequencing; cfDNA: Cell-Free DNA; PCR; polymerase chain reaction; WES: Whole Exome Sequencing; NE: Not-Evaluable; NA: Not Applicable

Supplementary Material

Refer to Web version on PubMed Central for supplementary material.

Acknowledgements

We thank the patients and their families for participating in this study. This work was supported by Genentech and grants from the Histiocyte Society, the Erdheim-Chester Disease Global Alliance, the Functional Genomics Initiative of Memorial Sloan Kettering Cancer Center (MSKCC), the Society of Memorial Sloan Kettering Cancer Center, the Histiocytosis Association, the Translational and Integrative Medicine Award of Memorial Sloan Kettering Cancer Center, the Geoffrey Beene Center of MSKCC, the American Society of Hematology, the Leukemia & Lymphoma Society, Frame Fund, Nonna's Garden Foundation, and National Institutions of Health (P30 CA008748, 1 R01 CA201247, K08 CA218901).

The authors report the following competing financial and non-financial interests: The authors declare the following competing interests: DLH: grants from Erdheim-Chester Disease Global Alliance, The Histiocytosis Association, the Society of Memorial Sloan Kettering, and the American Society for Clinic Oncology. BHD: grants from National Cancer Institute, American Society of Hematology, and Erdheim-Chester Disease Global Alliance Foundation. GU: personal fees from Sanofi and grants from Sanofi, Novartis, Genentech. RJY: personal fees from Agios, PUMA, NordicNeuroLabs and Icon, and grants from Agios. RR: personal fees from Incyte, Celgene, Agios, Jazz, BeyondSpring, Apexx, and Partner Therapeutics, and research funding from Stemline and Constellation. ML: personal fees and royalties from Roche/Genentech, and research funding from Veloce, Berg, US Biotest. AD: personal fees from Roche, Corvus Pharmaceuticals, Physicians' Education Resource, Seattle Genetics, Peerview Institute, Oncology Specialty Group, Pharmacyclics, Celgene, and Novartis and grants from National Cancer Institute, Roche. NR: personal fees from Array BioPharma, Millennium Pharmaceuticals, AstraZeneca / MedImmune, Novartis, Eli Lilly, Boehringer Ingelheim, Merrimack Pharmaeutics, Chugai, Beigene, Daiichi Sankyo, Kura Oncology, ZAI Lab, F-Prime, and Kadmon and grants from Chugai, Bayer, and Tarveda. AI: personal fees from Mylan. OAW: grants from National Cancer Institute, National Heart Lung and Blood Institute, and H3B Biomedicine and personal fees from H3B Biomedicine, Foundation Medicine Inc, Merck, and Jansen. DMH: personal fees from Atara Biotherapeutics, Chugai Pharma, Boehringer Ingelheim, AstraZeneca, Pfizer, Bayer, Debiopharm Group, and Genetech, and grants from National Cancer Institute, AstraZeneca, Puma Biotechnology, and Loxo Oncology. The remaining authors have nothing to disclose.

References

1. Haroche J et al. Histiocytoses: emerging neoplasia behind inflammation. The Lancet. Oncology 18, e113–e125, doi:10.1016/S1470-2045(17)30031-1 (2017). [PubMed: 28214412]
2. Allen CE, Merad M & McClain KL Langerhans-Cell Histiocytosis. The New England journal of medicine 379, 856–868, doi:10.1056/NEJMra1607548 (2018). [PubMed: 30157397]
3. Badalian-Very G et al. Recurrent BRAF mutations in Langerhans cell histiocytosis. Blood 116, 1919–1923, doi:10.1182/blood-2010-04-279083 (2010). [PubMed: 20519626]

4. Haroche J et al. High prevalence of BRAF V600E mutations in Erdheim-Chester disease but not in other non-Langerhans cell histiocytoses. Blood 120, 2700–2703, doi:10.1182/blood-2012-05-430140 (2012). [PubMed: 22879539]
5. Emile JF, Charlotte F, Amoura Z & Haroche J BRAF mutations in Erdheim-Chester disease. Journal of clinical oncology : official journal of the American Society of Clinical Oncology 31, 398, doi:10.1200/JCO.2012.46.9676 (2013). [PubMed: 23248255]
6. Hyman DM et al. Vemurafenib in Multiple Nonmelanoma Cancers with BRAF V600 Mutations. N Engl J Med 373, 726–736, doi:10.1056/NEJMoa1502309 (2015). [PubMed: 26287849]
7. Diamond EL et al. Vemurafenib for BRAF V600-Mutant Erdheim-Chester Disease and Langerhans Cell Histiocytosis: Analysis of Data From the Histology-Independent, Phase 2, Open-label VE-BASKET Study. JAMA Oncol 4, 384–388, doi:10.1001/jamaoncol.2017.5029 (2018). [PubMed: 29188284]
8. Diamond EL et al. Diverse and Targetable Kinase Alterations Drive Histiocytic Neoplasms. Cancer Discov 6, 154–165, doi:10.1158/2159-8290.CD-15-0913 (2016). [PubMed: 26566875]
9. Brown NA et al. High prevalence of somatic MAP2K1 mutations in BRAF V600E-negative Langerhans cell histiocytosis. Blood 124, 1655–1658, doi:10.1182/blood-2014-05-577361 (2014). [PubMed: 24982505]
10. Chakraborty R et al. Mutually exclusive recurrent somatic mutations in MAP2K1 and BRAF support a central role for ERK activation in LCH pathogenesis. Blood 124, 3007–3015, doi:10.1182/blood-2014-05-577825 (2014). [PubMed: 25202140]
11. Emile JF et al. Recurrent RAS and PIK3CA mutations in Erdheim-Chester disease. Blood 124, 3016–3019, doi:10.1182/blood-2014-04-570937 (2014). [PubMed: 25150293]
12. Nelson DS et al. Somatic activating ARAF mutations in Langerhans cell histiocytosis. Blood 123, 3152–3155, doi:10.1182/blood-2013-06-511139 (2014). [PubMed: 24652991]
13. Chakraborty R et al. Alternative genetic mechanisms of BRAF activation in Langerhans cell histiocytosis. Blood 128, 2533–2537, doi:10.1182/blood-2016-08-733790 (2016). [PubMed: 27729324]
14. Cohen Aubart F et al. Targeted therapies in 54 patients with Erdheim-Chester disease, including follow-up after interruption (the LOVE study). Blood 130, 1377–1380, doi:10.1182/blood-2017-03-771873 (2017). [PubMed: 28667012]
15. Jacobsen E, Shanmugam V & Jagannathan J Rosai-Dorfman Disease with Activating KRAS Mutation - Response to Cobimetinib. N Engl J Med 377, 2398–2399, doi:10.1056/NEJMc1713676 (2017). [PubMed: 29236635]
16. Gounder MM, Solit DB & Tap WD Trametinib in Histiocytic Sarcoma with an Activating MAP2K1 (MEK1) Mutation. N Engl J Med 378, 1945–1947, doi:10.1056/NEJMc1511490 (2018). [PubMed: 29768143]
17. Diamond EL et al. Consensus guidelines for the diagnosis and clinical management of Erdheim-Chester disease. Blood 124, 483–492, doi:10.1182/blood-2014-03-561381 (2014). [PubMed: 24850756]
18. Abla O et al. Consensus recommendations for the diagnosis and clinical management of Rosai-Dorfman-Destombes disease. Blood 131, 2877–2890, doi:10.1182/blood-2018-03-839753 (2018). [PubMed: 29720485]
19. Allen CE, Ladisch S & McClain KL How I treat Langerhans cell histiocytosis. Blood 126, 26–35, doi:10.1182/blood-2014-12-569301 (2015). [PubMed: 25827831]
20. Eisenhauer EA et al. New response evaluation criteria in solid tumours: revised RECIST guideline (version 1.1). Eur J Cancer 45, 228–247, doi:10.1016/j.ejca.2008.10.026 (2009). [PubMed: 19097774]
21. Arnaud L et al. CNS involvement and treatment with interferon-alpha are independent prognostic factors in Erdheim-Chester disease: a multicenter survival analysis of 53 patients. Blood 117, 2778–2782, doi:10.1182/blood-2010-06-294108 (2011). [PubMed: 21239701]
22. Rosen LS et al. A first-in-human phase I study to evaluate the MEK1/2 inhibitor, cobimetinib, administered daily in patients with advanced solid tumors. Invest New Drugs 34, 604–613, doi:10.1007/s10637-016-0374-3 (2016). [PubMed: 27424159]

23. Larkin J et al. Combined vemurafenib and cobimetinib in BRAF-mutated melanoma. N Engl J Med 371, 1867–1876, doi:10.1056/NEJMoa1408868 (2014). [PubMed: 25265494]
24. Falchook GS et al. Activity of the oral MEK inhibitor trametinib in patients with advanced melanoma: a phase 1 dose-escalation trial. Lancet Oncol 13, 782–789, doi:10.1016/S1470-2045(12)70269-3 (2012). [PubMed: 22805292]
25. Pratilas CA et al. Genetic predictors of MEK dependence in non-small cell lung cancer. Cancer research 68, 9375–9383, doi:10.1158/0008-5472.CAN-08-2223 (2008). [PubMed: 19010912]
26. Solit DB et al. BRAF mutation predicts sensitivity to MEK inhibition. Nature 439, 358–362, doi:10.1038/nature04304 (2006). [PubMed: 16273091]
27. Gao Y et al. Allele-Specific Mechanisms of Activation of MEK1 Mutants Determine Their Properties. Cancer discovery 8, 648–661, doi:10.1158/2159-8290.CD-17-1452 (2018). [PubMed: 29483135]
28. Emery CM et al. MEK1 mutations confer resistance to MEK and B-RAF inhibition. Proceedings of the National Academy of Sciences of the United States of America 106, 20411–20416, doi:10.1073/pnas.0905833106 (2009). [PubMed: 19915144]
29. Cheng DT et al. Memorial Sloan Kettering-Integrated Mutation Profiling of Actionable Cancer Targets (MSK-IMPACT): A Hybridization Capture-Based Next-Generation Sequencing Clinical Assay for Solid Tumor Molecular Oncology. The Journal of molecular diagnostics : JMD 17, 251–264, doi:10.1016/j.jmoldx.2014.12.006 (2015). [PubMed: 25801821]
30. Durham BH et al. Genomic analysis of hairy cell leukemia identifies novel recurrent genetic alterations. Blood, doi:10.1182/blood-2017-01-765107 (2017).
31. Zheng Z et al. Anchored multiplex PCR for targeted next-generation sequencing. Nat Med 20, 1479–1484, doi:10.1038/nm.3729 (2014). [PubMed: 25384085]

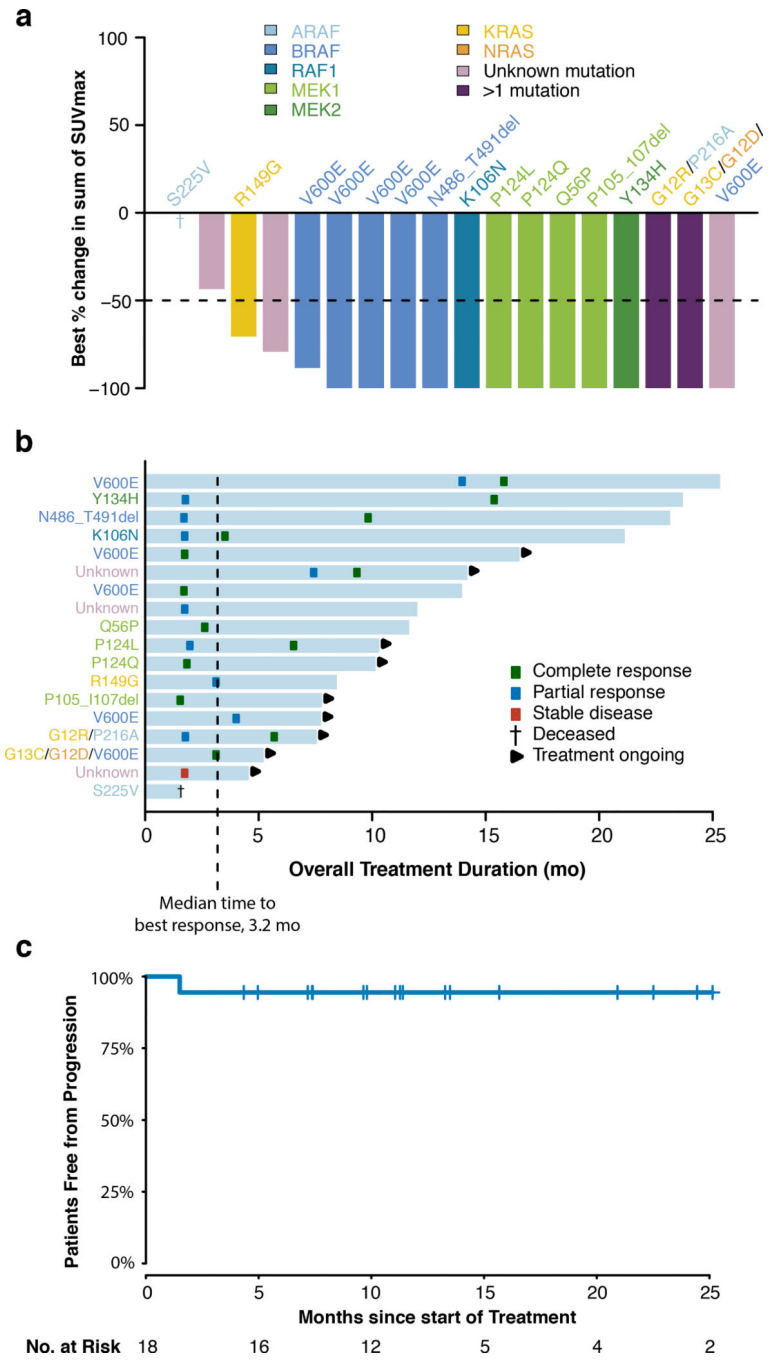

Figure 1: Efficacy of MEK1/2 inhibition with cobimetinib across molecular subtypes of histiocytoses.

(a) Waterfall plot of the maximum change in tumor metabolism according to standardized uptake values (SUVs) measured by positron emission tomography (PET). Colors of bars indicate genomic alteration present. Notations above bars indicate specific mutation. One patient (dagger) died due to underlying disease prior to first response evaluation. The lower dotted lines represent cut-off for partial response. **(b)** Swimmer plot of outcomes in all 18 patients. **(c)** PET-Defined progression-free survival (n=18).

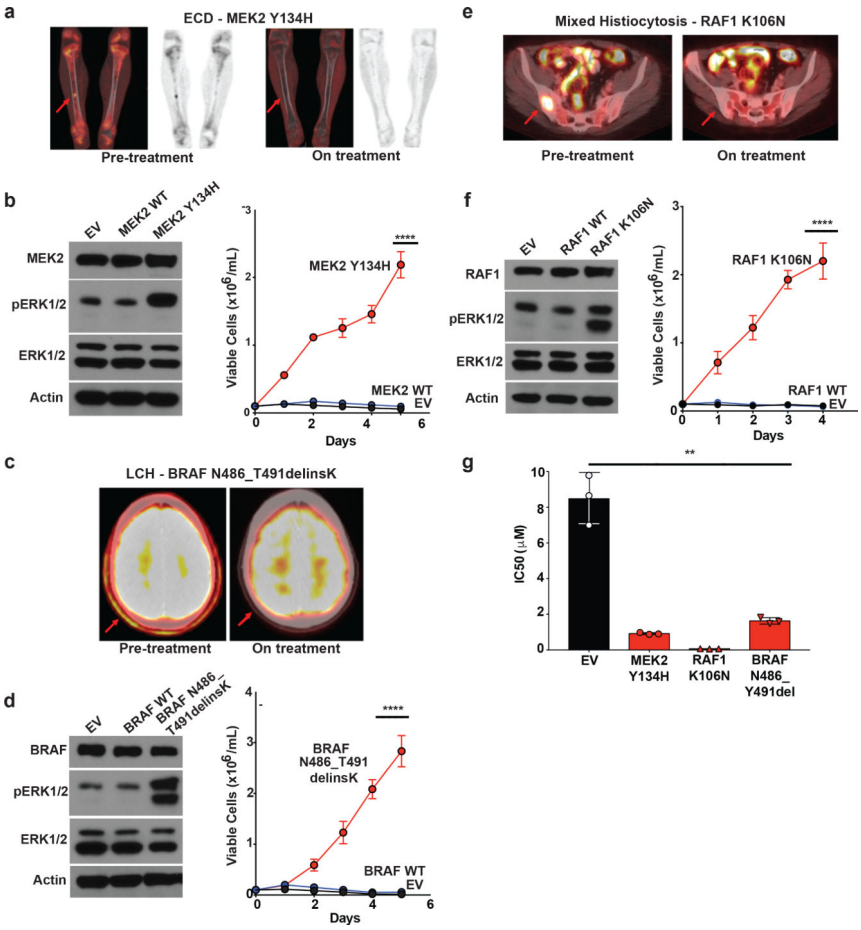

Figure 2: Characterization of novel activating mutations in MEK2, RAF1, and BRAF and their dependence on ERK signaling in histiocytoses.

(a) Coronal PET and fused PET/CT imaging of femurs showing characteristic femoral lesions of ECD from a MEK2 Y134H mutant ECD patient pre- and during cobimetinib treatment. **(b)** Western blot (left) and number of viable cells (right) following IL-3 withdrawal of Ba/F3 cells stably expressing an empty vector, wild-type (WT) MEK2, or MEK2 Y134H mutant (the average of n=3 biological replicates ± standard deviation (SD) is plotted). Calculation of *p*-values was performed using two-way ANOVA; ****$p<0.0001$. **(c)** Axial fused PET/CT imaging showing skull lesions (arrow) pre- and during cobimetinib treatment in a patient with BRAF N486_T491delinsK mutant LCH. **(d)** Western blot (left) and number of viable cells (right) following IL-3 withdrawal of Ba/F3 cells stably expressing an empty vector, WT BRAF, or BRAF N486_T491delinsK mutant (the average of n=3 biological replicates ± SD is plotted). Calculation of *p*-values was performed using two-way ANOVA; ****$p<0.0001$. **(e)** Axial fused PET/CT imaging showing sacral lesions (arrow) pre-and during cobimetinib treatment in a patient with mixed histiocytosis and a RAF1 K106N mutation. **(f)** Western blot (left) and number of viable cells (right) following IL-3 withdrawal of Ba/F3 cells stably expressing an empty vector, WT RAF1, or RAF1 K106N mutant (the average of n=3 biological replicates ± SD is plotted). Calculation of *p*-values was performed using two-way ANOVA; ****$p<0.0001$. **(g)** IC_{50} of cells from (b), (d), and (e) to 72 hours of cobimetinib. Each experiment was performed with n=3 biological

replicates and average ± SD is plotted. The calculation of *p*-values utilized the Ordinary one-way ANOVA; $^{**}p < 0.01$.